

## Neuropeptide Y is a critical modulator of Leptin's regulation of cortical bone

Iris PL Wong,<sup>1,2</sup> Amy D Nguyen,<sup>1</sup> Ee Cheng Khor,<sup>1,2</sup> Ronaldo F Enriquez,<sup>1,2</sup> John A Eisman,<sup>2,3</sup> Amanda Sainsbury,<sup>1,4</sup> Herbert Herzog,<sup>1,3\*</sup> and Paul A Baldock<sup>1,2,3</sup>

<sup>1</sup>Neuroscience Program, Garvan Institute of Medical Research, St Vincent's Hospital, Sydney, Australia

<sup>2</sup>Osteoporosis and Bone Biology, Garvan Institute of Medical Research, St Vincent's Hospital, Sydney, Australia

<sup>3</sup>Faculty of Medicine, University of New South Wales, Sydney, Australia <sup>4</sup>School of Medical Sciences, University of New South Wales, Sydney, Australia

### Abstract

Leptin signaling is required for normal bone homeostasis; however, loss of leptin results in differing effects on cortical and cancellous bone, as well as altered responses between the axial and appendicular regions. Local  $\beta$ -adrenergic actions are responsible for the greater cancellous bone volume in leptin-deficient (*ob/ob*) mice; however, the mechanism responsible for the opposing reduction in cortical bone in *ob/ob* mice is not known. Here we show that blocking the leptin-deficient increase in neuropeptide Y (NPY) expression reverses the cortical bone loss in *ob/ob* mice. Mice null for both NPY and leptin (NPY-/-*ob/ob*), display greater cortical bone mass in both long-bones and vertebra, with NPY-/-*ob/ob* mice exhibiting thicker and denser cortical bone, associated with greater endocortical and periosteal mineral apposition rate (MAR), compared to *ob/ob* animals. Importantly, these cortical changes occurred without significant increases in body weight, with NPY-/-*ob/ob* mice showing significantly reduced adiposity compared to *ob/ob* controls, most likely due to the reduced respiratory exchange ratio seen in these animals. Interestingly, cancellous bone volume was not different between NPY-/-*ob/ob* and *ob/ob*, suggesting that NPY is not influencing the adrenergic axis. Taken together, this work demonstrates the critical role of NPY signaling in the regulation of bone and energy homeostasis, and more importantly, suggests that reduced leptin levels or leptin resistance, which occurs in obesity, could potentially inhibit cortical bone formation via increased central NPY signaling.

---

### Introduction

Both the neuropeptide Y (NPY) and the leptin systems have been identified to be important central regulators of bone and energy metabolism. However, their differing effect on bone indicates significant differences in their action. Leptin deficiency has opposing effects on cancellous and cortical bone. Although cancellous bone volume is greater in leptin-deficient (*ob/ob*) compared to normal mice,<sup>1, 2</sup> *ob/ob* mice have shorter stature and reduced whole-body bone mineral density (BMD), bone mineral content (BMC), cortical area, and mineralizing surface of the femur.<sup>3, 4</sup> In addition to envelope-specific effects, *ob/ob* mice also display altered responses between the axial and appendicular regions. *ob/ob* Mice were found to have increased vertebral length, lumbar BMD, and cancellous bone volume, but shorter femur length, femoral BMD, and cortical thickness, compared to lean wild-type mice.<sup>5</sup>

In contrast to the effects of leptin deficiency, the lack of NPY signaling has consistent anabolic effects in both cancellous and cortical bone through increased osteoblast activity. NPY deletion in mice results in greater cancellous bone volume at the distal femur and lumbar vertebrae as well as thicker cortical bone, whereas viral-mediated overexpression of NPY, specifically in the hypothalamus, markedly decreases bone mass and bone formation.<sup>2, 6</sup> The major receptor through which NPY mediates these effects on bone is the Y1 receptor,<sup>7, 8</sup> with bone formation being inhibited by Y1 receptors expressed on osteoblasts.<sup>9, 10</sup>

Interestingly, the activity of these two systems has a close association within the hypothalamus, with NPY an important downstream effector of leptin signaling. An inverse relationship exists between leptin and NPY; expression of NPY is elevated in the hypothalamus following a reduction in leptin due to starvation<sup>11-13</sup> and in *ob/ob* mice,<sup>14, 15</sup> whereas administration of leptin to *ob/ob* mice reduces the elevated levels of NPY.<sup>16, 17</sup> This increase in

NPY is an important component of the leptin pathway. Central injection of NPY mimics many of the characteristics of leptin deficiency, including hyperphagia, hyperinsulinemia, decreased thermogenesis, and the development of obesity.<sup>18, 19</sup> These findings suggest a commonality in mechanism between the NPY and the leptin systems in energy metabolism. However, the interaction between these two systems on bone metabolism is not fully understood.

Our recent studies in mouse models with elevated NPY levels in the hypothalamus suggest that NPY may in fact be mediating part of the skeletal phenotype observed in *ob/ob* mice,<sup>2, 6</sup> acting in addition to the beta-adrenergic sympathetic pathway originating from the ventromedial hypothalamus that modulates cancellous bone in these mice.<sup>20</sup> NPY overexpression in the arcuate nucleus of the hypothalamus of wild-type mice, which mimics the elevated NPY levels seen in *ob/ob* mice, not only replicated the marked increase in body weight but also the diminished long-bone mass observed in *ob/ob* mice, with associated reduction in endocortical mineral apposition rate (MAR).<sup>6</sup> Importantly, there is one major difference between *ob/ob* and NPY overexpressed mice: the presence of leptin. However, despite this difference, the skeletal phenotype was similar, most notably in cortical bone, with a marked decrease in long-bone mass observed in both models despite different leptin levels. This result indicates that the bone mass reduction in *ob/ob* mice may result from the specific increase in NPY in the hypothalamus. Thus, we hypothesized that, in *ob/ob* mice, although the central beta-adrenergic actions accounts for the greater cancellous bone volume,<sup>1, 20</sup> the diminished cortical bone may be due to elevated hypothalamic NPY expression. To examine the interactions between these two systems and the direct contributions of elevated NPY on the skeletal phenotype of *ob/ob*, leptin/NPY dual-deficient mice were generated (NPY<sup>-/-ob/ob</sup>) and compared with *ob/ob* mice, for changes in bone morphology and bone cell activities, with particular emphasis on cortical bone. Body weight, body composition, and metabolic parameters that influence them were also measured in these mice in order to determine the possible contribution of any changes in energy balance to the observed changes in bone.

## Subjects and Methods

### Animals

All research and animal care procedures were approved by the Garvan Institute/St Vincent's Hospital Animal Experimentation Ethics Committee and conducted in accordance with the Australian Code of Practice for the Care and Use of Animals for Scientific Purpose. Mice were housed under conditions of controlled temperature (22°C) with a 12-hour light, 12-hour dark cycle (lights on at 7:00 a.m.). Mice were fed a normal chow diet *ad libitum* (8% calories from fat, 21% calories from protein, 71% calories from carbohydrate, 2.6 kcal/g; Gordon's Speciality Stock Feeds, Yanderra, New South Wales, Australia). Water was available *ad libitum* for all mice.

NPY-deficient *ob/ob* mice (NPY<sup>-/-ob/ob</sup>) were generated by crossing male NPY<sup>-/-</sup> mice<sup>6</sup> on a mixed C57BL/6-129/SvJ background with female heterozygous (*OB/ob*) mice that were on C57BL/6. Double heterozygous (NPY<sup>+/-OB/ob</sup>) animals were crossed again to subsequently obtain all of the nine possible genotypes. The *ob* genotype was determined by restriction fragment-length polymorphism analysis using *DdeI* enzyme on a 496-bp PCR product generated from genomic DNA isolated from these mice with primer set A (5'-GAGTCAAGCATTGTGGAGT-3') and B (5'-CAGTCGGTATCCGCCAAG-3'), as described.<sup>21</sup>

### Food intake

In *ob/ob*, NPY<sup>-/-ob/ob</sup>, and wild-type mice of both genders, spontaneous food intake was measured at 11 and 19 weeks of age whereas fasting-induced food intake was measured at 12 weeks of age, as described.<sup>22</sup> Briefly, mice were transferred from group housing on soft bedding to individual cages with paper towel bedding and allowed to acclimatize for 3 days. Food intake was measured daily over 3 consecutive days and was calculated as the weight of pellets taken from the food hopper minus the weight of food spillage in the cage.

### Indirect calorimetry

Indirect calorimetry studies were carried out on *ob/ob*, NPY<sup>-/-ob/ob</sup>, and wild-type littermates of both genders at 14 to 15 weeks of age as described.<sup>23</sup> Briefly, the metabolic rate was measured by indirect calorimetry using an eight-chamber open-circuit calorimeter (Oxymax Series; Columbus Instruments, Columbus, OH, USA). Preweighed mice were housed individually in specially built Plexiglas cages (20.1 × 10.1 × 12.7 cm). Temperature was maintained at 22°C

with airflow of 0.6 L/min. Food and water were available *ad libitum*. Mice were acclimatized to the cages for 24 hours before a subsequent 24 hours of monitoring in the system. Oxygen consumption (VO<sub>2</sub>) and carbon dioxide production (VCO<sub>2</sub>) were measured every 27 minutes. The respiratory exchange ratio (RER) was calculated as the quotient of VCO<sub>2</sub>/VO<sub>2</sub>, with 100% carbohydrate oxidation resulting in an RER of 1 and 100% fat oxidation resulting in an RER of 0.7. **24, 25** Energy expenditure (kcal heat produced) was calculated as Calorific Value (CV) × VO<sub>2</sub>, where CV is 3.815 + 1.232 × RER. **26** Data for the 24-hour monitoring period was averaged for 1-hour intervals for energy expenditure (kcal/h) and RER.

#### *Measurement of physical activity*

While the mice were within the metabolic cages, physical activity was recorded continuously by infrared beam sensors using an OPTO-M3 sensor system with a 60-second data download interval (Columbus Instruments) at the same time as the indirect calorimetric measurements. This system provides both total counts (every time a beam is broken) and ambulatory counts (when consecutive adjacent beams are broken) in the *x* and *y* directions. The recording of ambulatory counts does not include the same beam being broken repeatedly and thus measures actual locomotion. Therefore, ambulatory counts in the *x* and *y* directions were used to measure physical activity, and continuous recording of individual mouse data were summed for 1-hour intervals.

#### *Bone densitometry and body composition analysis*

Whole-body BMC, BMD, fat mass, and nonfat non-bone mass (hereafter referred to as "lean mass") were measured on isoflurane-anesthetized mice, ventral side down with head and tail exclusion, using a dedicated mouse dual-energy X-ray absorptiometry (DXA) device (Lunar Piximus II; GE Medical Systems, Madison, WI, USA), as described. **6**

#### *Micro-computed tomography*

Micro-computed tomography (microCT), using the Skyscan 1174 scanner and associated analysis software (Skyscan, Aartselaar, Belgium), was used to examine three-dimensional bone structure, as described. **27** Following fixation, bone was packed into an enclosed rigid plastic tube filled with 70% ethanol. To reduce beam hardening, a 0.5-mm aluminum filter was applied with the X-ray source set to maximum (50 kV), exposure time set to 3600 ms, and sharpening set to 40%. Distal femora were scanned at (6.2- $\mu$ m pixel size) and acquired over an angular range of 180 degrees, with a rotation step of 0.4 degrees. The image projections were reconstructed using NRecon (Skyscan's volumetric reconstruction software). Reconstruction was carried out with automated misalignment compensation, beam-hardening correction set to 30%, ring artifact correction set to 5, smoothing set to 4, and the threshold for defect pixel masking set to 10%. The reconstructed images were then aligned using Dataviewer software (Skyscan).

Analyses of the cortical bone were carried out in 150 slices (0.93 mm) selected at 730 slices (4.53 mm) proximal from the distal femoral growth plate using CT-Analyzer software (Skyscan). The following parameters were generated: total cross-sectional area, cortical bone area, marrow area, cortical area fraction, cortical bone thickness, periosteal perimeter, endosteal perimeter, and mean polar moment of inertia (a basic index of strength). Additionally, BMD was measured in reconstructed grayscale images. Gray values were calibrated as material density using two phantoms of hydroxyapatite-resin with mineral concentration of 0.25 g/cm<sup>3</sup> and 0.75 g/cm<sup>3</sup>. Bone material density was then calculated as the average mineral density within the bone profiles.

For vertebrae, a landmark was identified at each end of the third vertebral body, defined by the disappearance of cartilage at the growth plate. Slices between the rostral and caudal landmarks were selected, with 10 slices offset from the rostral landmark and 25 slices offset from the caudal landmark. Vertebrae bodies in the selected slices were then separated from the vertebral processes using an elliptical region of interest. This isolated vertebrae body was then subdivided into cancellous and cortical part by manual tracing. Cancellous bone volume was generated for the cancellous region of the third lumbar vertebral body.

#### *Tissue collection and bone histomorphometry*

Upon completion of the study, mice were euthanized at 16 or 24 weeks of age by cervical dislocation and decapitation between 12:00 p.m. and 5:00 p.m. for collection of trunk blood. Serum was separated by centrifugation and stored at -20°C. Serum corticosterone was measured

using radioimmunoassay detection kits from MP Biomedicals (Irvine, CA, USA), whereas serum insulin growth factor 1 (IGF-1) was measured using a radioimmunoassay detection kit from Bioclone (Sydney, Australia).

For bone analysis both femora were excised and fixed in 4% PBS-buffered paraformaldehyde for 16 hours at 4°C. The right femora were bisected transversely at the midpoint of the long axis. After dehydration, distal halves were embedded un-decalcified in methyl-methacrylate (Medim-Medizinische Diagnostik, Giessen, Germany).

Sagittal sections of 5 µm thickness were stained and evaluated as described.**28** Analysis of cancellous bone volume (BV/TV, %), trabecular thickness (Tb.Th, µm), and trabecular number (Tb.N, mm<sup>-1</sup>) was carried out on sections stained with modified von Kossa for mineralized bone. To access bone formation indices, mice were given subcutaneous injections of the fluorescent compound calcein (Sigma Chemical Company, St. Louis, MO, USA), 20 mg/kg at 10 and 3 days prior to collection. Mineralizing surface (MS, %) and MAR (µm/d) were measured from unstained sections and bone formation rate (BFR = MS/BS × MAR; µm<sup>2</sup>/µm/d) were calculated. Bone resorption indices—osteoclast surface (Oc.S, %) and number (Oc.N, mm<sup>-1</sup>)—were estimated in tartrate-resistant acid phosphatase-stained sections.**29** All cancellous measurements were conducted in a sample area bordering the epiphyseal growth plate, beginning 0.25 mm proximal to the mineralization zone to exclude primary spongiosa and extending proximally 4.2 mm, encompassing all the cancellous bone within the cortices, as described.**8** The cortical mineral apposition rate was measured at the mid-point of the shaft on the posterior endosteal surface in a region 1000 µm proximal from the mid-femora.

#### *Statistical analysis*

Statistical analyses were performed in GraphPad Prism 5 (Version 5.0a, GraphPad Software, Inc., San Diego, CA, USA) using two-tailed Student's *t* test between the two obese models: NPY<sup>-/-</sup>/*ob/ob* and *ob/ob*. For all statistical analyses, *p* values below 0.05 were considered to be statistically significant, and error bars represent SEM.

## **Results**

#### *Lack of NPY reduces adiposity and increases BMD in ob/ob mice*

DXA analysis was used to measure body composition in NPY<sup>-/-</sup>/*ob/ob* and *ob/ob* mice. This revealed significantly reduced fat mass in NPY<sup>-/-</sup>/*ob/ob* compared to *ob/ob* mice (Fig. 1A, B), associated with a slight reduction in body weight in female mice. In males, a significant change in body composition was evident, with an increase in lean mass countering any loss of body weight. When adjusted for body weight, NPY<sup>-/-</sup>/*ob/ob* mice of both genders had lower percentage fat mass and greater percentage lean mass than *ob/ob* (Table 1). The lower fat content of NPY<sup>-/-</sup>/*ob/ob* was confirmed by weighing discrete white adipose tissue depots (inguinal, mesenteric, retroperitoneal, and reproductive—epididymal in males, parametrial in females). The combined weight of the four adipose tissue depots was significantly lower in male NPY<sup>-/-</sup>/*ob/ob* than *ob/ob* mice, with the same trend also observed in female mice (Fig. 2A, B). Similarly, the greater lean mass of male NPY<sup>-/-</sup>/*ob/ob* mice measured by DXA was confirmed by the weight of discrete muscle tissues (tibialis anterior, gastrocnemius, soleus, and extensor digitorum longus [EDL]), demonstrating that NPY ablation attenuates the sarcopenia of *ob/ob* mice.**30** Compared to *ob/ob* mice, male NPY<sup>-/-</sup>/*ob/ob* mice had a trend toward greater combined weight of the four muscle tissues (Fig. 2C, D), which was significant when expressed as a percentage of body weight (Table 1).

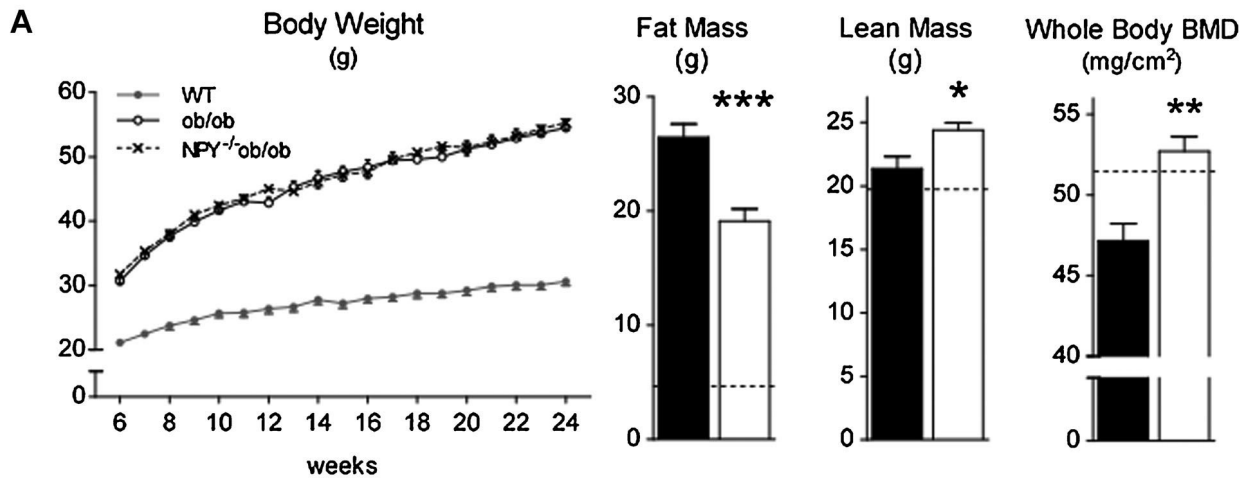
Despite similar or lower body weight compared to *ob/ob* mice, NPY<sup>-/-</sup>/*ob/ob* mice had greater whole-body BMD in males and females (Fig. 1). The skeletal phenotype of NPY<sup>-/-</sup>/*ob/ob* mice was further examined in detail, with cortical and cancellous compartments analyzed separately, using histomorphometry and microCT.

#### *NPY deletion in ob/ob mice improves femoral cortical bone*

Femurs from NPY<sup>-/-</sup>/*ob/ob* mice were significantly longer than those from *ob/ob* mice (Fig. 3), attenuating the well-documented reduced stature of *ob/ob* mice. In addition, as detailed below, NPY deletion improved cortical bone of *ob/ob* mice in terms of structure, material, and bone cell activities, consistent with the hypothesis that NPY plays a role in the diminished cortical bone of *ob/ob* mice.

**MALE**

■ *ob/ob* □ *NPY<sup>-/-ob/ob</sup>*



**FEMALE**

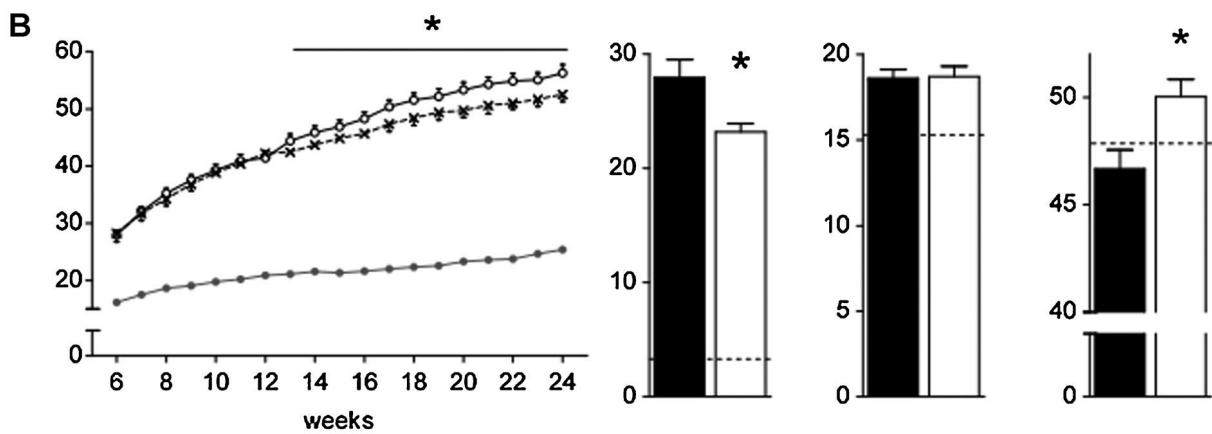


**Fig. 1.** NPY deletion reduces body adiposity and increases whole-body BMD of *ob/ob* mice. (A) Body weight was not different between male *NPY<sup>-/-ob/ob</sup>* and *ob/ob* mice, but a shift in body composition was observed in 16-week-old male *NPY<sup>-/-ob/ob</sup>* relative to *ob/ob* mice, with lower fat mass, greater lean mass, and increased whole-body BMD as measured by DXA. (B) Reduced fat mass and greater whole-body BMD were also evident in 16-week-old female *NPY<sup>-/-ob/ob</sup>* mice compared to *ob/ob* mice, with significantly lower body weight observed starting from 13 weeks of age. As reference, lean wild-type controls (WT) are shown as a gray line in body weight curve and a dotted black line in bar graphs. Mean  $\pm$  SEM of 6 to 20 mice per group are shown. \* $p < 0.05$ ; \*\* $p < 0.005$ ; \*\*\* $p < 0.001$  between *NPY<sup>-/-ob/ob</sup>* versus *ob/ob* mice.

**Table 1.** Effects of NPY Deletion on Adiposity and Muscle Mass in 16-Week-Old *ob/ob* Mice, Expressed as a Percentage of Body Weight

Males	WT (n = 4)	<i>ob/ob</i> (n = 6)	NPY <sup>-/-</sup> <i>ob/ob</i> (n = 13)
Summed white adipose mass (%BW)	2.9 ± 0.2	9.2 ± 0.3	7.8 ± 0.3*
Retroperitoneal white adipose mass (%BW)	0.27 ± 0.04	0.63 ± 0.05	0.52 ± 0.03
Epididymal white adipose mass (%BW)	1.0 ± 0.1	2.4 ± 0.2	2.5 ± 0.1
Mesenteric white adipose mass (%BW)	0.88 ± 0.08	3.2 ± 0.2	2.7 ± 0.1*
Inguinal white adipose mass (%BW)	0.74 ± 0.01	2.9 ± 0.2	2.0 ± 0.1***
Whole-body fat mass (%BW) <sup>a</sup>	17.2 ± 1.2	52.5 ± 1.6	40.5 ± 1.3***
Summed muscle mass (%BW)	0.74 ± 0.02	0.32 ± 0.02	0.39 ± 0.01**
Soleus muscle mass (%BW)	0.030 ± 0.002	0.016 ± 0.001	0.017 ± 0.001
Extensor digitorum longus muscle mass (%BW)	0.034 ± 0.002	0.016 ± 0.000	0.019 ± 0.001 <sup>0.06</sup>
Tibialis anterior muscle mass (%BW)	0.156 ± 0.010	0.064 ± 0.004	0.088 ± 0.003***
Gastrocnemius muscle mass (%BW)	0.52 ± 0.01	0.23 ± 0.01	0.27 ± 0.01*
Whole-body lean mass (%BW) <sup>a</sup>	74.4 ± 1.2	42.3 ± 1.5	52.2 ± 1.1***
Females	WT (n = 7)	<i>ob/ob</i> (n = 7)	NPY <sup>-/-</sup> <i>ob/ob</i> (n = 10)
Summed white adipose mass (%BW)	2.4 ± 0.1	11.4 ± 0.4	10.8 ± 0.5 <sup>0.10</sup>
Retroperitoneal white adipose mass (%BW)	0.12 ± 0.01	0.57 ± 0.04	0.60 ± 0.08
Parametrial white adipose mass (%BW)	0.78 ± 0.07	4.0 ± 0.2	4.4 ± 0.3
Mesenteric white adipose mass (%BW)	0.72 ± 0.06	3.6 ± 0.1	3.3 ± 0.1
Inguinal white adipose mass (%BW)	0.74 ± 0.05	3.2 ± 0.3	2.4 ± 0.2*
Whole-body fat mass (%BW) <sup>a</sup>	16.1 ± 0.6	56.9 ± 1.2	51.7 ± 0.8**
Summed muscle mass (%BW)	0.76 ± 0.02	0.28 ± 0.01	0.30 ± 0.01
Soleus muscle mass (%BW)	0.029 ± 0.002	0.014 ± 0.001	0.016 ± 0.001
Extensor digitorum longus muscle mass (%BW)	0.034 ± 0.001	0.013 ± 0.001	0.016 ± 0.001
Tibialis anterior muscle mass (%BW)	0.166 ± 0.005	0.058 ± 0.002	0.075 ± 0.006*
Gastrocnemius muscle mass (%BW)	0.53 ± 0.01	0.19 ± 0.01	0.20 ± 0.01
Whole-body lean mass (%BW) <sup>a</sup>	73.8 ± 0.4	38.1 ± 1.0	41.7 ± 0.8*

Means ± SEM shown with the number of mice per group in bracket.

NPY = neuropeptide Y; *ob/ob* = leptin-deficient; WT = wild-type; NPY<sup>-/-</sup> *ob/ob* = NPY-deficient leptin-deficient; BW = body weight;

<sup>a</sup>DXA measurements with head and tail exclusion.

\**p* < 0.05 between NPY<sup>-/-</sup> *ob/ob* versus *ob/ob*.

\*\**p* < 0.005 between NPY<sup>-/-</sup> *ob/ob* versus *ob/ob*.

\*\*\**p* < 0.001 between NPY<sup>-/-</sup> *ob/ob* versus *ob/ob*. Superscripted values are *p* values between NPY<sup>-/-</sup> *ob/ob* versus *ob/ob*.

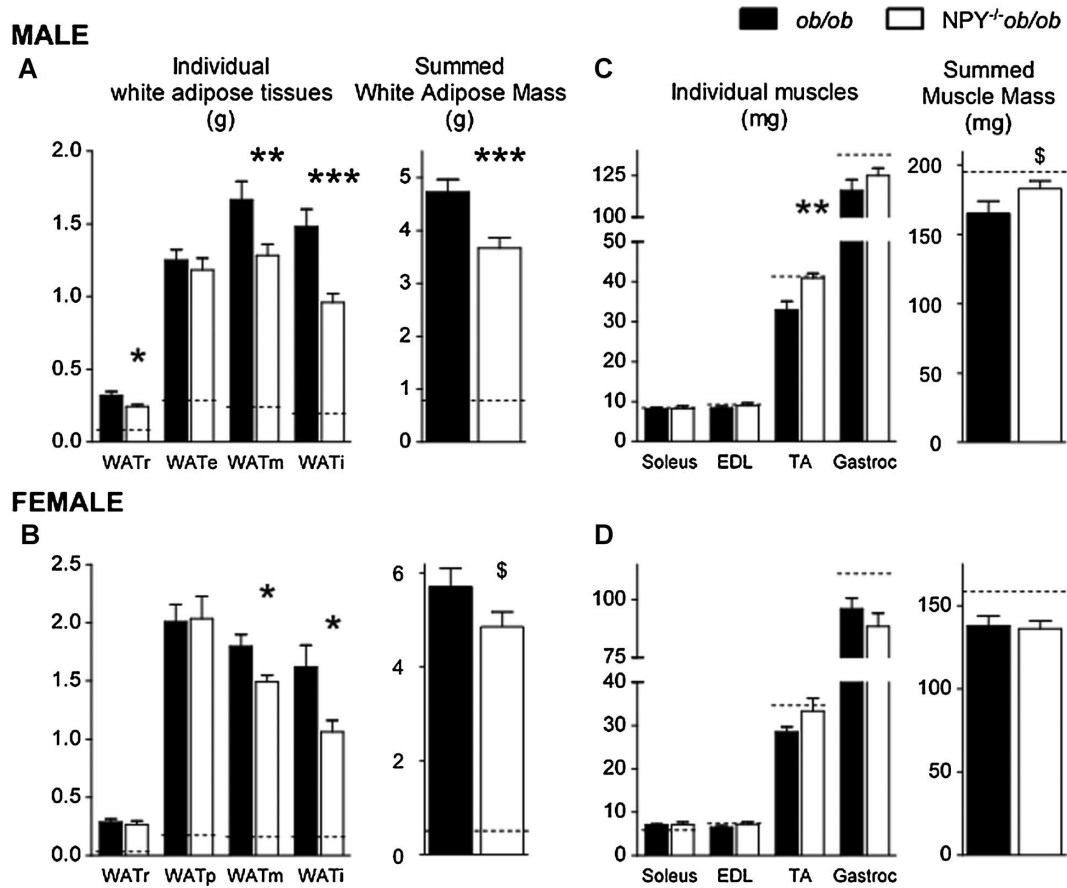


**Fig. 2.** Dissected adipose and muscle weights recapitulate DXA findings of *ob/ob* and *NPY<sup>-/-</sup>ob/ob* mice. (A, B) Mass of individual white adipose depots, namely retroperitoneal (WATr), epididymal (WATe), mesenteric (WATm), inguinal (WATi), and combined weight of these depots in 16-week-old *ob/ob* and *NPY<sup>-/-</sup>ob/ob* mice of both genders. (C, D) Mass of individual muscles, namely soleus, extensor digitorum longus (EDL), tibialis anterior (TA), gastrocnemius (Gastroc), and combined weight of these muscles in 16-week-old *ob/ob* and *NPY<sup>-/-</sup>ob/ob* mice of both genders. As reference, lean wild-type controls (WT) are shown by dotted black line. Mean  $\pm$  SEM of 6 to 13 mice per group are shown. \* $p < 0.05$ ; \*\* $p < 0.005$ ; \*\*\* $p < 0.001$  for *NPY<sup>-/-</sup>ob/ob* versus *ob/ob* mice.

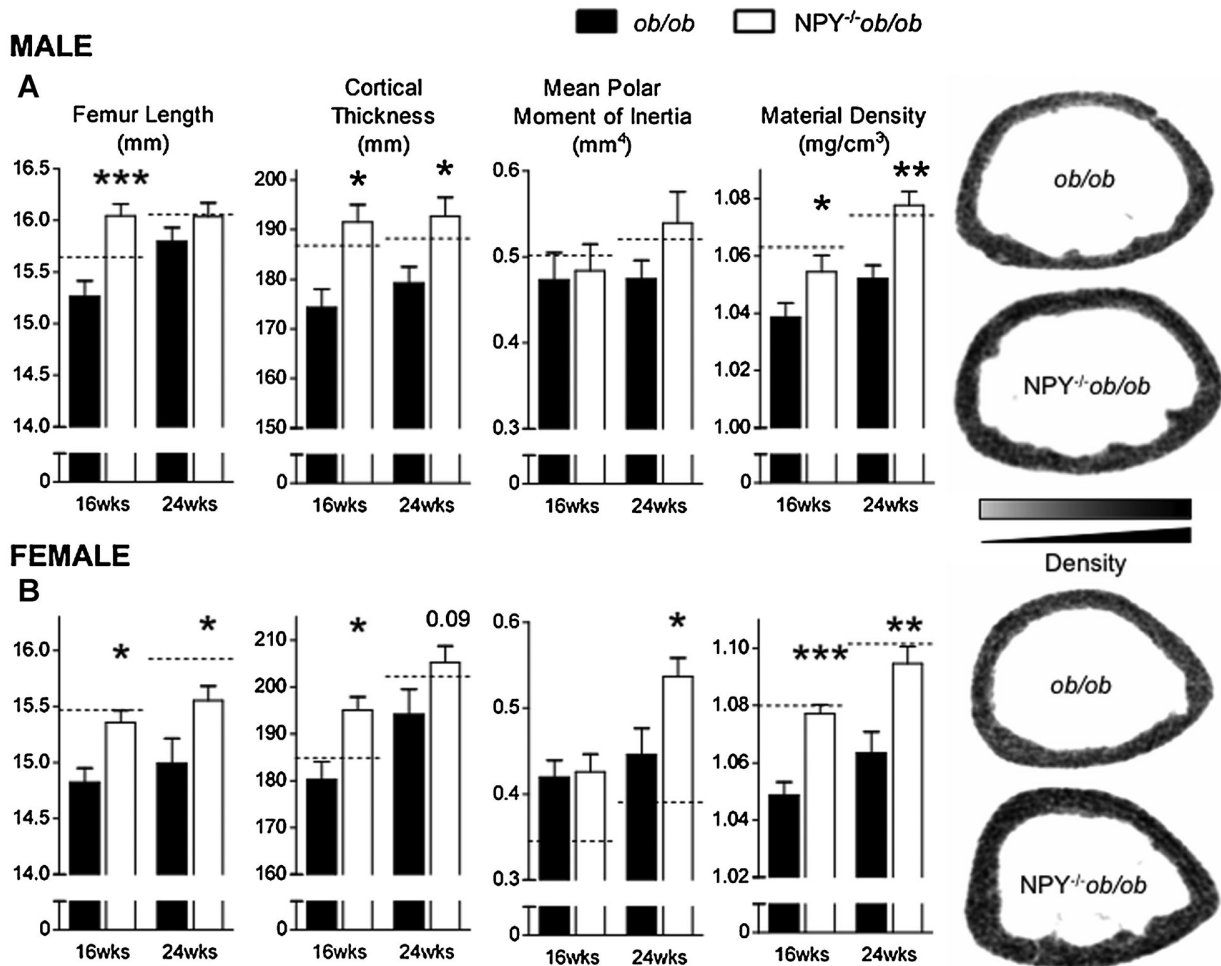


**Fig. 3.** (A, B) Removal of NPY in *ob/ob* mice results in greater cortical thickness, improved cortical structure, and increased material density. NPY<sup>-/-</sup>*ob/ob* mice had longer femur and thicker cortical bone than *ob/ob*. At 24 weeks of age, mean polar moment of inertia, a basic strength index, was greater in female NPY<sup>-/-</sup>*ob/ob* than in *ob/ob* mice. NPY deletion also increases cortical bone material density in *ob/ob* to level indifferent from wild-type irrespective of gender and age, illustrated by the density heat map of 24-week-old mice. As reference, the value for lean wild-type controls (WT) is shown as a dotted black line. Means  $\pm$  SEM of 7 to 13 mice per group are shown. \* $p < 0.05$ ; \*\* $p < 0.005$ ; \*\*\* $p < 0.001$  for NPY<sup>-/-</sup>*ob/ob* versus *ob/ob* mice.

*Structure: thicker cortical bone in NPY<sup>-/-</sup>ob/ob mice*

At 16 weeks of age, cortical bone was thicker in both male and female NPY<sup>-/-</sup>*ob/ob* mice than in *ob/ob* mice (Fig. 3) with no change in tissue area or periosteal perimeter (Supplementary Table 1). At 24 weeks of age, cortical bone of NPY<sup>-/-</sup>*ob/ob* mice remained thicker than that of *ob/ob* mice (Fig. 3). Tissue area, cortical bone area, and mean polar moment of inertia were significantly greater in 24-week-old female NPY<sup>-/-</sup>*ob/ob* mice than in *ob/ob* mice, and a similar trend was observed in 24-week-old male mice (Fig. 3, Supplementary Table 2).

*Material: NPY deletion rescues the lower bone material density in ob/ob mice*

In addition to the structural differences, our study also highlights material differences between cortical bone of NPY<sup>-/-</sup>*ob/ob* and *ob/ob* mice, with cortical bone material density greater in NPY<sup>-/-</sup>*ob/ob* compared to *ob/ob* mice (Fig. 3), indicating denser mineral per unit volume of bone. This increase in bone material density in NPY<sup>-/-</sup>*ob/ob* mice is evident in both genders at



both ages examined (Fig. 3).

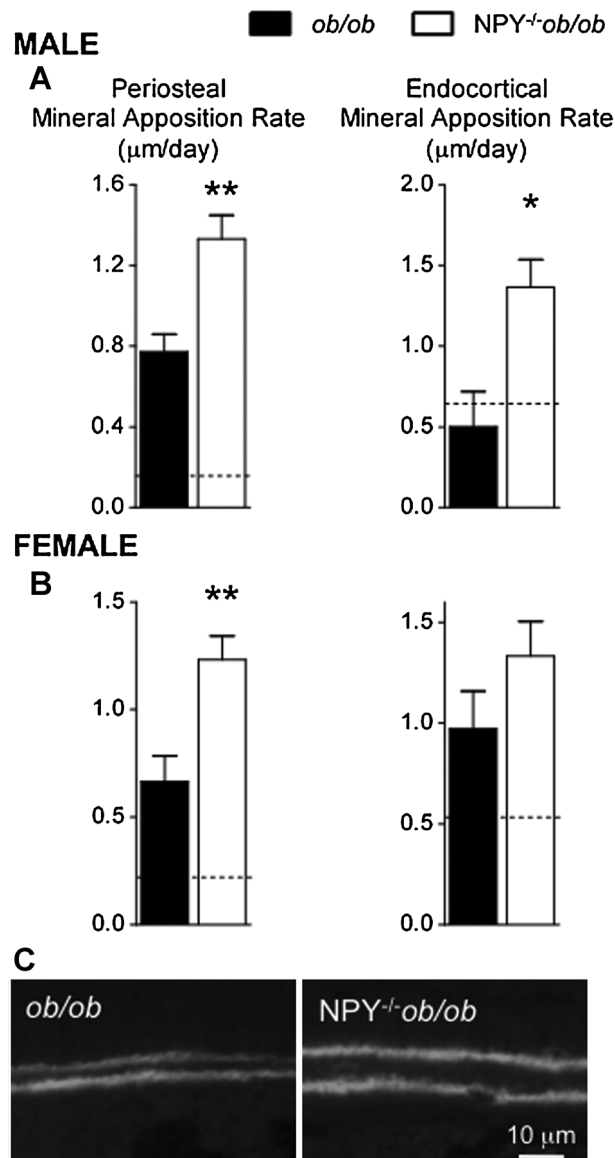


**Fig. 4.** Greater cortical mineral apposition rate in *NPY<sup>-/-</sup>ob/ob* compared to *ob/ob* mice. (A, B) Both periosteal and endocortical mineral apposition rates are greater in 16-week-old *NPY<sup>-/-</sup>ob/ob* than in *ob/ob* mice. Though not significant, a similar trend was observed in endocortical mineral apposition rate of female *NPY<sup>-/-</sup>ob/ob* mice. As reference, the value for lean wild-type controls (WT) is shown as a dotted black line. (C) Representative photomicrographs of endocortical MAR of male mice (scale bar = 10  $\mu\text{m}$ ). Means  $\pm$  SEM of 8 to 13 mice per group shown. \* $p < 0.05$ ; \*\* $p < 0.005$  for *NPY<sup>-/-</sup>ob/ob* versus *ob/ob* mice.

*Bone cell activity: greater cortical mineral apposition rate in *NPY<sup>-/-</sup>ob/ob* mice*

To examine in more detail the cellular basis for the thicker cortical bone observed in *NPY<sup>-/-</sup>ob/ob* mice, fluorescent histomorphometry was used to visualize cortical bone formation at the mid-femur in sagittal sections (Fig. 4). Cortical mineral apposition rates were generally greater in both knockout genotypes compared to wild-type, most notably on periosteal surfaces, consistent with their substantially greater body weight. However, they were further elevated in *NPY<sup>-/-</sup>ob/ob* compared to *ob/ob* mice, at both endosteal and periosteal sites, despite similar or lower body weight of *NPY<sup>-/-</sup>ob/ob* mice compared to *ob/ob* mice.

*NPY deletion does not alter femoral cancellous bone*

Having shown that deletion of NPY improves multiple aspects of cortical bone in *ob/ob* mice, cancellous bone was also examined. At the distal femur, cancellous bone volume was not different between *ob/ob* and *NPY<sup>-/-ob/ob</sup>* mice of both genders (Fig. 5), indicating that the difference observed in DXA is not attributable to difference in cancellous bone. Interestingly, bones from male *NPY<sup>-/-ob/ob</sup>* mice had a lower trabecular thickness relative to *ob/ob* mice (*NPY<sup>-/-ob/ob</sup>*  $29.5 \pm 0.9$  versus *ob/ob*  $35.1 \pm 1.1$   $\mu\text{m}$ ,  $p < 0.001$ ), suggesting potential alterations in cancellous bone cell activities.

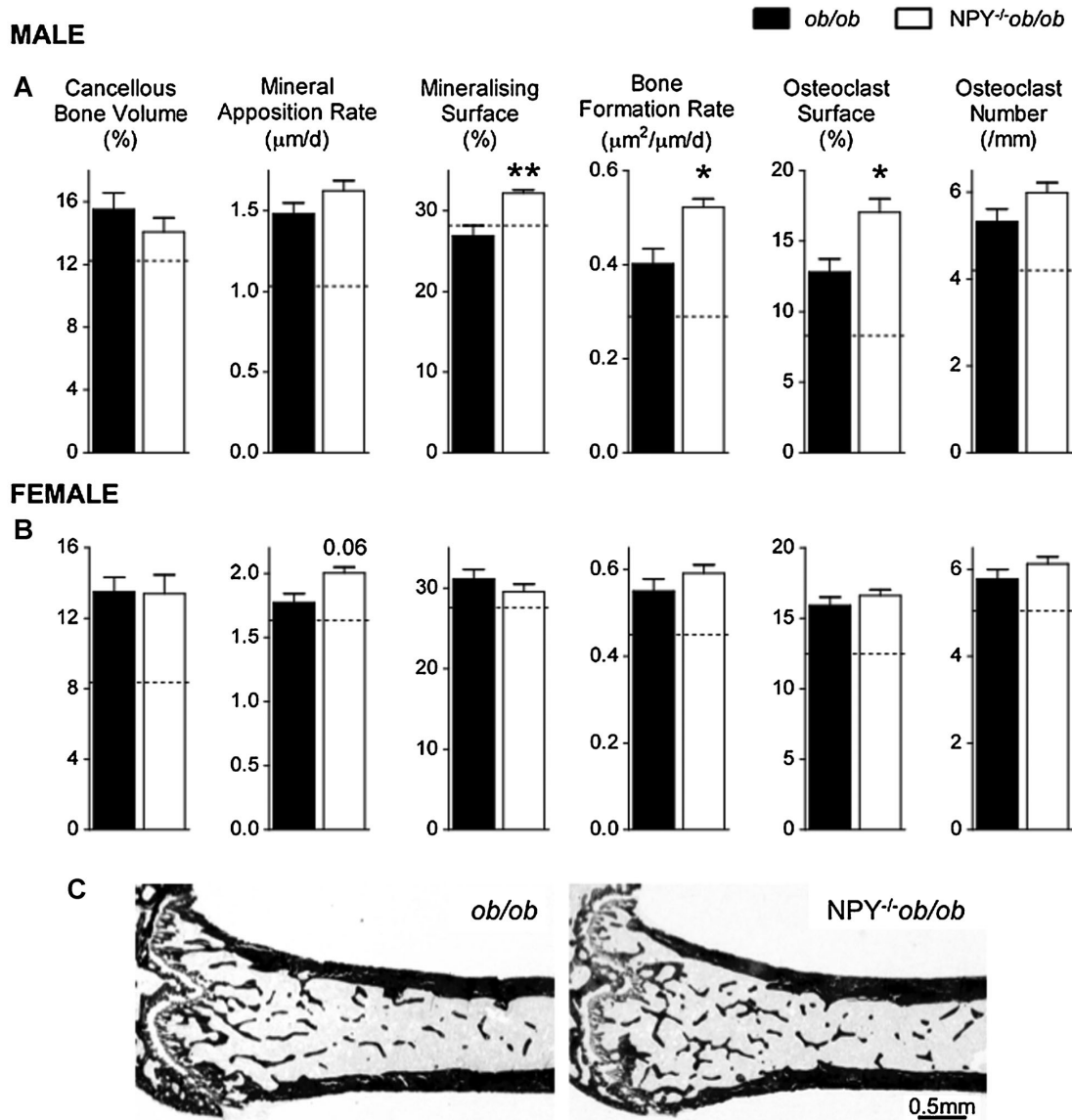


**Fig. 5.** Similar cancellous bone volume between *NPY<sup>-/-ob/ob</sup>* and *ob/ob* mice despite alteration in bone cell activities in male mice. (A) Despite similar cancellous bone volume, 16-week-old male *NPY<sup>-/-ob/ob</sup>* mice have greater bone turnover, as evidenced by the greater mineralizing surface, bone formation rate, and osteoclast surface, compared to *ob/ob*. (B) Female *NPY<sup>-/-ob/ob</sup>* mice are similar to *ob/ob* in terms of cancellous bone volume and all parameters of cancellous bone formation and resorption measured except for a slight trend toward a greater mineral apposition rate. As reference, the value for lean wild-type controls (WT) is shown as a dotted black line. (C) Representative photomicrographs of sagittal distal femoral section of male mice (scale bar = 0.5 mm). Means  $\pm$  SEM of 5 to 13 mice per group are shown. <sup>§</sup> $p < 0.06$ , \* $p < 0.05$ ; \*\* $p < 0.005$  for *NPY<sup>-/-ob/ob</sup>* versus *ob/ob* mice.

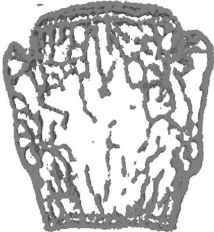
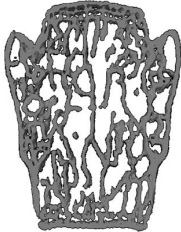
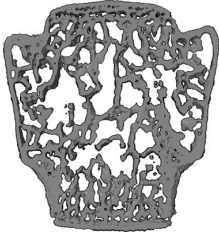
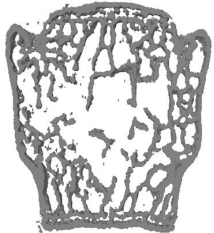
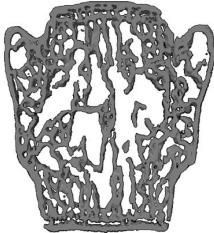
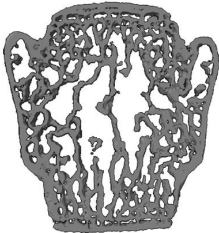
Interestingly, bone turnover in male *NPY<sup>-/-ob/ob</sup>* mice, was mildly but significantly elevated compared to *ob/ob* mice, with greater mineralizing surface, bone formation rate, and osteoclast surface (Fig. 5). These alterations in cancellous bone cell activities mirror that of NPY knockout mice relative to wild-type,<sup>6</sup> and may reflect the supraphysiological reduction in NPY in *NPY<sup>-/-ob/ob</sup>* mice rather than a true correction to wild-type levels. This suggests that, at least in male mice, leptin and NPY may regulate bone homeostasis via distinct pathways. In contrast,

trabecular structure (data not shown) and cancellous bone cell activities (Fig. 5) did not differ between female NPY<sup>-/-ob/ob</sup> and *ob/ob* mice, apart from a trend toward greater MAR in NPY<sup>-/-ob/ob</sup> mice.

*Vertebral effects of NPY deletion in ob/ob mice*

To examine whether axial and appendicular bone were affected in a similar manner, cortical and cancellous bone of the lumbar vertebrae were examined. Findings from microCT analysis of the lumbar vertebral body demonstrated similarities similar to those observed in the femur (Table 2). Cortical bone of the vertebral body was thicker in NPY<sup>-/-ob/ob</sup> than in *ob/ob* mice of both genders. Similar to the cortical phenotype, cancellous bone volume in the lumbar vertebral body was not significantly different between *ob/ob* and NPY<sup>-/-ob/ob</sup> mice in both genders (Table 2). The greater vertebral length of *ob/ob* mice was not altered by NPY deletion, as a result, cortical bone volume was greater than in the wild-type in *ob/ob* and NPY<sup>-/-ob/ob</sup> mice. Despite numerically similar changes between genders, cortical area was greater in NPY<sup>-/-ob/ob</sup> mice compared to *ob/ob* mice in females only. In cancellous bone the greater BV/TV of *ob/ob* mice was evident in both genders, and, as in femur, was not altered by NPY deletion, with no differences between *ob/ob* and NPY<sup>-/-ob/ob</sup> mice.

**Table 2.** Bone Phenotype in Lumbar Vertebral Body of *ob/ob* and NPY<sup>-/-ob/ob</sup> Mice

	WT	<i>ob/ob</i>	NPY <sup>-/-ob/ob</sup>
<b>Males</b>			
Lumbar vertebral body			
Vertebral height (mm)	2.08 ± 0.01*	2.43 ± 0.06**	2.55 ± 0.03**
<b>Cancellous</b>			
BV/TV (%)	23.9 ± 0.6*	32.1 ± 0.8**	32.3 ± 1.4**
Tb.Th (μm)	54.8 ± 0.4*	61.0 ± 0.5**	60.9 ± 0.5**
Tb.N (mm <sup>-1</sup> )	4.36 ± 0.14*	5.26 ± 0.11**	5.29 ± 0.19**
<b>Cortical</b>			
Bone.Vol (mm <sup>3</sup> )	0.74 ± 0.01*	0.89 ± 0.03**	0.98 ± 0.02**,*
Cort.Th (μm)	80.6 ± 0.8	79.7 ± 0.6	83.9 ± 1.1*
<b>Females</b>			
Lumbar vertebral body			
Vertebral height (mm)	1.92 ± 0.05*	2.49 ± 0.07**	2.52 ± 0.03**
<b>Cancellous</b>			
BV/TV (%)	19.04 ± 0.05*	31.4 ± 0.5**	29.8 ± 1.9**
Tb.Th (μm)	53.9 ± 0.4*	61.0 ± 0.4**	61.0 ± 0.6**
Tb.N (mm <sup>-1</sup> )	3.53 ± 0.16*	5.15 ± 0.06**	4.87 ± 0.27**
<b>Cortical</b>			
Bone.Vol (mm <sup>3</sup> )	0.66 ± 0.01*	0.89 ± 0.05**	0.98 ± 0.04**
Cort.Th (μm)	84.3 ± 0.5	79.7 ± 1.3	86.6 ± 1.9*

At 16 weeks of age, cortical bone is thicker in NPY<sup>-/-ob/ob</sup> than in *ob/ob* mice, whereas cancellous bone remains unaltered in the lumbar vertebral body of both genders. Values are mean ± SEM of 5 to 6 mice per group shown.

*ob/ob* = leptin-deficient; NPY<sup>-/-ob/ob</sup> = neuropeptide Y-null, leptin deficient; BV/TV = bone volume/total volume; Tb.Th = trabecular thickness; Tb.N = trabecular number; Bone.Vol = bone volume; Cort.Th = cortical thickness; WT = wild-type.

\**p* < 0.05 versus *ob/ob*.

\*\**p* < 0.05 versus WT.

*Metabolic and hormonal parameters affected by NPY deletion in ob/ob mice*

Having established the skeletal phenotype of NPY<sup>-/-ob/ob</sup> and *ob/ob* mice in this study, metabolic and hormonal parameters were examined to identify potential changes that may contribute to the observed effects on adiposity and skeletal homeostasis.

*Metabolic: altered substrate utilization in NPY<sup>-/-ob/ob</sup> mice, no change in activity*

Food intake at 11 weeks of age (Table 3) and fasting-induced food intake at 12 weeks of age (Table 4) were not different between *ob/ob* and NPY<sup>-/-ob/ob</sup> mice. At 19 weeks of age, when a lower body weight was apparent in female NPY<sup>-/-ob/ob</sup> compared to *ob/ob* mice, food consumption was significantly lower in NPY<sup>-/-ob/ob</sup> mice (Table 3). However, when adjusted for body weight, no significant difference in food intake was observed between *ob/ob* and NPY<sup>-/-ob/ob</sup> mice (Table 3). Physical activity was dramatically decreased in both leptin-deficient mouse models compared to wild-type, consistent with the reduced energy expenditure in these models of central starvation. Importantly, however, physical activity was not different between NPY<sup>-/-ob/ob</sup> and *ob/ob* mice (Fig. 6A, B). To identify whether alterations in substrate utilization may be associated with the reduced adiposity in NPY<sup>-/-ob/ob</sup> relative to *ob/ob* mice, respiratory exchange ratio (RER), an index of oxidative fuel source, was calculated as the quotient of VCO<sub>2</sub>/VO<sub>2</sub>, with 100% carbohydrate oxidation resulting in an RER of 1 and 100% fat oxidation resulting in an RER of 0.7. **24, 25** Male NPY<sup>-/-ob/ob</sup> mice exhibited significant reductions in overall RER compared to *ob/ob* mice, suggesting a greater use of lipid as an oxidative fuel source and/or reduced lipogenesis (Fig. 6C, D). In female NPY<sup>-/-ob/ob</sup> mice, the reduced RER was only significant in the light period (Fig. 6C, D). This finding, when combined with our observation of a slight reduction in food consumption, may contribute to the lower adiposity of NPY<sup>-/-ob/ob</sup> relative to *ob/ob* mice. Taken together, these data indicate that deletion of NPY in *ob/ob* mice alters substrate utilization, favoring the use of lipid as an oxidative fuel source, as indicated by the reduced RER, and this may contribute to the reduced adiposity observed. However, importantly, differences in physical activity cannot explain the alterations in cortical bone between NPY<sup>-/-ob/ob</sup> and *ob/ob* mice.

**Table 3.** Spontaneous Food Intake of *ob/ob* and NPY<sup>-/-ob/ob</sup> Mice

	Males			Females		
	WT (n = 7)	<i>ob/ob</i> (n = 6)	NPY <sup>-/-ob/ob</sup> (n = 11)	WT (n = 8)	<i>ob/ob</i> (n = 9)	NPY <sup>-/-ob/ob</sup> (n = 11)
11 weeks old						
Body weight (g)	26.0 ± 0.7	42.6 ± 1.2	44.5 ± 0.9	20.4 ± 0.2	42.0 ± 0.9	41.4 ± 0.9
Food intake (g/d)	3.98 ± 0.09	4.94 ± 0.11	4.80 ± 0.12	3.82 ± 0.12	4.57 ± 0.13	4.48 ± 0.08
Food intake (%BW)	15.3 ± 0.2	11.6 ± 0.2	10.8 ± 0.3 <sup>0.07</sup>	18.7 ± 0.6	10.9 ± 0.3	10.8 ± 0.2
19 weeks old						
	WT (n = 7)	<i>ob/ob</i> (n = 6)	NPY <sup>-/-ob/ob</sup> (n = 11)	WT (n = 7)	<i>ob/ob</i> (n = 7)	NPY <sup>-/-ob/ob</sup> (n = 12)
Body weight (g)	29.2 ± 0.7	51.9 ± 1.3	50.0 ± 1.2	22.4 ± 0.3	52.4 ± 1.3	48.1 ± 1.0*
Food intake (g/d)	4.33 ± 0.36	6.27 ± 0.65	4.71 ± 0.20 <sup>0.06</sup>	4.06 ± 0.17	5.13 ± 0.18	4.48 ± 0.18*
Food intake (%BW)	14.8 ± 1.1	12.1 ± 1.3	9.5 ± 0.4 <sup>0.10</sup>	18.1 ± 0.6	9.8 ± 0.3	9.4 ± 0.5

Means ± SEM of 6 to 12 mice per group shown.

*ob/ob* = leptin-deficient; NPY<sup>-/-ob/ob</sup> = neuropeptide Y-deficient leptin-deficient; WT = wild-type; BW = body weight.

\**p* < 0.05 between NPY<sup>-/-ob/ob</sup> versus *ob/ob*. Superscripted values are *p* values between NPY<sup>-/-ob/ob</sup> versus *ob/ob*.

*Hormonal: NPY deletion improves fertility and reduces serum corticosterone levels in ob/ob mice*

The hypothalamo-pituitary-gonadotropic axis is known to be inhibited by hypothalamic NPY administration or leptin deficiency. **31-33** In the present study, fertility was regained in otherwise infertile male *ob/ob* mice by the absence of NPY, although increases in seminal vesicle and testes weight compared to *ob/ob* mice did not reach significance (data not shown). Five of eight male NPY<sup>-/-ob/ob</sup> mice paired with fertile females (*ob/+* and NPY<sup>+/-ob/+</sup>) were able to produce offspring, as opposed to one of eight *ob/ob* mice. Fertility in female NPY<sup>-/-ob/ob</sup> mice was not examined, but the combined weight of ovaries and uterus in female NPY<sup>-/-ob/ob</sup> was greater than in *ob/ob* mice (NPY<sup>-/-ob/ob</sup> 79 ± 10 mg versus *ob/ob* 35 ± 5 mg, *p* < 0.005). Serum

corticosterone levels were lower in NPY<sup>-/-ob/ob</sup> than in *ob/ob* mice of both genders (male: NPY<sup>-/-ob/ob</sup> 146 ± 27 ng/mL versus *ob/ob* 288 ± 56 ng/mL, *p* < 0.05; female: NPY<sup>-/-ob/ob</sup> 195 ± 44 ng/mL versus *ob/ob* 343 ± 38 ng/mL, *p* < 0.05), potentially mediating the effect of NPY deletion on the skeleton (Table 5). Interestingly, serum concentrations of IGF-1 were unaffected (male: NPY<sup>-/-ob/ob</sup> 301 ± 18 ng/mL versus *ob/ob* 273 ± 45 ng/mL, *p* = not significant; female: NPY<sup>-/-ob/ob</sup> 251 ± 26 ng/mL versus *ob/ob* 250 ± 22 ng/mL, *p* = not significant) (Table 5), despite the observed increase in longitudinal bone growth (Fig. 3).

**Table 4.** Fasting-Induced Food Intake of *ob/ob* and NPY<sup>-/-ob/ob</sup> Mice

	Males			Females		
	WT (n = 7)	<i>ob/ob</i> (n = 6)	NPY <sup>-/-ob/ob</sup> (n = 11)	WT (n = 8)	<i>ob/ob</i> (n = 9)	NPY <sup>-/-ob/ob</sup> (n = 11)
Fasting-induced food intake (g)						
Hours post-re-feeding						
1	0.83 ± 0.05	0.94 ± 0.11	0.71 ± 0.11	0.80 ± 0.05	0.68 ± 0.07	0.53 ± 0.10
2	1.07 ± 0.08	1.24 ± 0.10	1.06 ± 0.10	0.96 ± 0.05	1.09 ± 0.07	0.86 ± 0.13
8	2.16 ± 0.14	2.21 ± 0.12	1.73 ± 0.15	2.07 ± 0.07	2.08 ± 0.12	1.79 ± 0.17
24	6.12 ± 0.23	5.88 ± 0.15	5.77 ± 0.22	5.68 ± 0.15	5.77 ± 0.20	5.59 ± 0.17
Fasting-induced food intake (%BW)						
Hours post-re-feeding						
1	3.8 ± 0.2	2.4 ± 0.2	1.7 ± 0.2	4.7 ± 0.3	1.7 ± 0.2	1.4 ± 0.3
2	4.9 ± 0.3	3.2 ± 0.3	2.6 ± 0.2	5.6 ± 0.3	2.7 ± 0.2	2.2 ± 0.3
8	9.8 ± 0.4	5.7 ± 0.3	4.2 ± 0.3	12.1 ± 0.4	5.2 ± 0.3	4.6 ± 0.4
24	28.1 ± 0.8	15.0 ± 0.2	14.3 ± 0.5	33.2 ± 0.9	14.5 ± 0.4	14.4 ± 0.5

Means ± SEM of 6 to 12 mice per group shown.

*ob/ob* = leptin-deficient; NPY<sup>-/-ob/ob</sup> = neuropeptide Y-deficient, leptin-deficient; WT = wild-type; BW = body weight.

\**p* < 0.05 versus *ob/ob*.

## Discussion

Studies surrounding the skeletal response to leptin have provided important new insights in the central regulation of bone mass. However, major aspects remain to be elucidated, including the mechanism behind the largest shift in bone mineral in the *ob/ob* mouse, the reduction in cortical bone mass. Our study demonstrates that the negative effects of leptin deficiency on cortical bone are modulated by NPY signaling. In particular, deletion of NPY in *ob/ob* mice, and thereby blocking the increase in hypothalamic NPY due to lack of leptin action, improved the cortical bone structure and bone material properties of *ob/ob* mice toward wild-type levels, irrespective of gender, sites (axial/appendicular) and age of the animal examined, and in the absence of any change in body weight that could explain the difference. Importantly, these data demonstrate that alterations in central NPY signaling can affect cortical bone mass and suggest that under conditions of negative energy balance the increase in central NPY levels contribute to diminished cortical bone mass; however, contributions from other factors cannot be excluded.

Leptin levels are directly correlated to levels of fat mass; therefore, anorexic conditions, which promote pronounced loss of fat, are associated with low leptin levels. This reduction in circulating leptin forms a fundamental component of the central perception of whole-body energy status. In this manner, reduced leptin signaling in the hypothalamus drives powerful starvation responses, including increased appetite and reduced energy expenditure. Similarly, the loss of leptin signaling in *ob/ob* mice also represents an anorexic model from the perspective of the brain, driving increased appetite and reduced energy expenditure, which produce the strong increase in fat mass. However, despite the increase in fat mass, leptin signaling remains defective and the starvation responses remain active. The low bone mass phenotype of the *ob/ob* mouse is therefore consistent with whole-body energy conservation subsequent to the central starvation signaling. NPY forms an important component of this central starvation signal, and specific overexpression of NPY in the hypothalamus recapitulates many aspects of the *ob/ob* model, including hyperphagia, and the development of obesity.<sup>18, 19, 34</sup> Indeed, we have previously employed a viral vector to induce continued NPY overexpression in the arcuate nucleus of the hypothalamus (as evident in *ob/ob*), while retaining intact leptin signaling.<sup>34</sup> In this manner, the activity of central NPY can be isolated and compared to leptin action throughout

the body. Viral mediated hypothalamic overexpression of NPY increases body weight by 75% and leptin by over twofold and, despite these changes, tibial bone mass is reduced by 20%,<sup>2, 35</sup> recapitulating the cortical phenotype of *ob/ob* mice, even with concurrent hyperleptinemia. This demonstrates the importance of central NPY to the regulation of bone mass and is consistent with the preservation of energy during episodes of starvation.

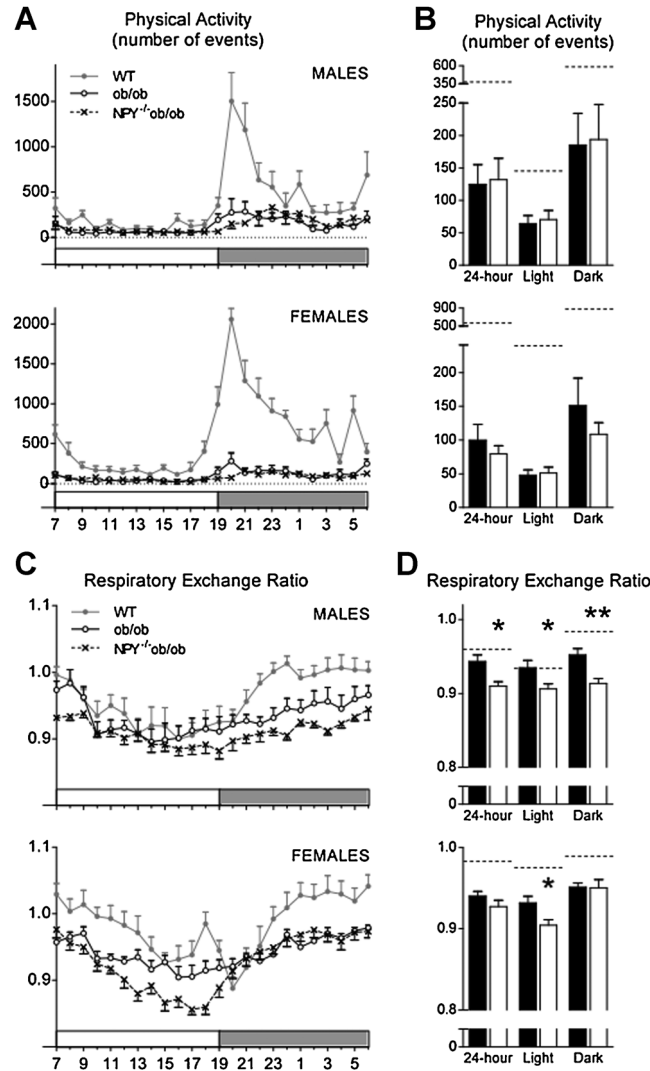


**Fig. 6.** *NPY<sup>-/-</sup>ob/ob* mice had increased fat oxidation and similar physical activity compared to *ob/ob* mice. Time course (A, C) and averages for 24-hour, light and dark phases (B, D) for respiratory exchange ratio, a measure of substrate utilization in A and B, and physical activity in C and D in wild-type (WT), *ob/ob*, and *NPY<sup>-/-</sup>ob/ob* mice of both genders. The gray line in A and C and dotted black line in B and D indicate reference values for lean wild-type controls (WT). Open and filled horizontal bars in A and C indicate light and dark phases, respectively. Means  $\pm$  SEM of 6 to 12 mice per group are shown. \**p* < 0.05; \*\**p* < 0.005 for *NPY<sup>-/-</sup>ob/ob* versus *ob/ob* mice.



**Table 5.** Serum Analyses of *ob/ob* and NPY<sup>-/-</sup> *ob/ob* Mice

	WT	<i>ob/ob</i>	NPY <sup>-/-</sup> <i>ob/ob</i>
<b>Males</b>			
Corticosterone (ng/mL)	133 ± 41	288 ± 56	146 ± 27*
IGF-1 (ng/mL)	185 ± 16	273 ± 45	312 ± 14
Testosterone (nmol/L)	1.84 ± 0.68	1.37 ± 1.14	0.30 ± 0.07
<b>Females</b>			
Corticosterone (ng/mL)	253 ± 28	343 ± 38	195 ± 44*
IGF-1 (ng/mL)	178 ± 18	250 ± 22	230 ± 18
Estradiol (pg/mL)	56.8 ± 11.5	72.3 ± 10.7	43.1 ± 11.2 <sup>0.10</sup>

Values are means ± SEM of mice per group shown.  
*ob/ob* = leptin-deficient; NPY<sup>-/-</sup> *ob/ob* = neuropeptide Y-deficient, leptin-deficient; WT = wild-type; IGF-1 = insulin growth factor 1.  
 \**p* < 0.05 between NPY<sup>-/-</sup> *ob/ob* versus *ob/ob*. Superscripted values are *p* values between NPY<sup>-/-</sup> *ob/ob* versus *ob/ob*.

Furthermore, a recent study<sup>36</sup> investigating the skeletal consequences of starvation showed that despite the expected reductions in body weight, fat, and bone mass caused by the restriction of caloric intake, cancellous bone volume of the spine was actually elevated, thus completely recapitulating the *ob/ob* phenotype, and the cortical effects of central NPY. The effects of altered central NPY on bone mass are far more pronounced in cortical than cancellous bone.<sup>35</sup> The expression profile of the local NPY receptor Y1R does not indicate a spatial explanation for this result<sup>37</sup>; however, loading is known to regulate NPY expression within osteoblastic cells, and a local load-responsive action may account for the greater sensitivity of cortical bone to NPY-mediated signaling.<sup>38</sup>

In comparison to the pronounced effects of NPY deletion observed in the cortical bone of *ob/ob* background in both genders, an alteration in cancellous bone was isolated to male mice. The already elevated cancellous bone turnover in male *ob/ob* mice was further increased in male NPY<sup>-/-</sup>*ob/ob* mice. Changes in osteoblast activity of NPY<sup>-/-</sup>*ob/ob* compared to *ob/ob* mirror that of NPY knockout mice relative to wild-type,<sup>6</sup> demonstrating distinct regulatory pathways of NPY and leptin on osteoblast activity in male mice. This is consistent with recent findings revealing distinct actions of leptin and Y2 receptor pathways on cancellous bone homeostasis as leptin levels increase to physiological levels.<sup>2</sup> Interestingly, in cancellous bone, these alterations in bone cell activities did not result in changes in bone volume, suggesting that increased hypothalamic NPY expression in *ob/ob* mice does not mediate the greater cancellous bone volume in these mice, consistent with previous studies indicating NPY being anti-anabolic to bone.<sup>6</sup>

NPY deletion has been reported to partly attenuate the obesity phenotype of *ob/ob* mice,<sup>39</sup> which could have also have effects on bone. In our NPY<sup>-/-</sup>*ob/ob* model the reduction in obesity was minor and did also not result in any alterations of serum parameters such as IGF-1, suggesting that the effects of NPY deletion on the skeletal phenotype of *ob/ob* mice are not attributable to changes in IGF-1. Conversely, enhanced gonadal function as indicated by the improved fertility and greater weight of reproductive organs as well as normalization of corticosterone levels in NPY<sup>-/-</sup>*ob/ob* compared to *ob/ob* mice may contribute to the observed skeletal phenotype. However, Y4 receptor deficient *ob/ob* mice, which also had normalized corticosterone levels and augmented gonadotropic function,<sup>35, 40</sup> did not exhibit parallel changes in bone like that observed in NPY-deficient *ob/ob*. Thus, these hormonal changes alone are not likely to contribute to the skeletal phenotype observed in NPY<sup>-/-</sup>*ob/ob* mice compared to *ob/ob*.

Together, this study clearly demonstrates a role of NPY in the diminished cortical bone of *ob/ob* mice, consistent with an action to conserve energy as a result of the central “perception” of starvation in *ob/ob* mice.<sup>6</sup> Conversely, the greater cancellous bone in *ob/ob* mice<sup>20</sup> may be a result of mineral sparing as a consequence of reduced cortical bone mass during negative energy balance, which had been shown previously in caloric restriction studies.<sup>36, 41</sup> Given that bone

strength to a large part is a function of the total bone mass,<sup>42</sup> in *ob/ob* mice, the NPY-mediated alterations in cortical bone mass may be more important than the  $\beta$ 2-adrenergic-mediated changes in cancellous bone mass.

### Acknowledgements

This work was supported by a grant from the NHMRC.

Authors' roles: Wong: Study concept and design; Data acquisition, analysis and interpretation; Statistical analysis; Manuscript preparation Khor: Data acquisition, analysis and interpretation; Statistical analysis; Manuscript preparation Nguyen and Enriquez: Data acquisition. Eisman: Data interpretation; Critical revision of the manuscript Sainsbury and Herzog: Study concept and design; Data interpretation; Critical revision of the manuscript; Baldock: Study concept and design; Data interpretation; Critical revision of the manuscript; Obtained funding and supervision.

### References

1. Ducy P, Amling M, Takeda S, Priemel M, Schilling AF, Beil FT, Shen J, Vinson C, Rueger JM, Karsenty G. Leptin inhibits bone formation through a hypothalamic relay: a central control of bone mass. *Cell*. 2000;100(2):197–207.
2. Baldock PA, Sainsbury A, Allison S, Lin EJ, Couzens M, Boey D, Enriquez R, During M, Herzog H, Gardiner EM. Hypothalamic control of bone formation: distinct actions of leptin and Y2 receptor pathways. *J Bone Miner Res*. 2005;20(10):1851–7.
3. Takeshita N, Mutoh S, Yamaguchi I. Osteopenia in genetically diabetic DB/DB mice and effects of 1 $\alpha$ -hydroxyvitamin D<sub>3</sub> on the osteopenia. Basic Research Group. *Life Sci*. 1995;56(13):1095–101.
4. Steppan CM, Crawford DT, Chidsey-Frink KL, Ke H, Swick AG. Leptin is a potent stimulator of bone growth in *ob/ob* mice. *Regul Pept*. 2000; 92(1–3):73–8.
5. Hamrick MW, Pennington C, Newton D, Xie D, Isaacs C. Leptin deficiency produces contrasting phenotypes in bones of the limb and spine. *Bone*. 2004;34(3):376–83.
6. Baldock PA, Lee NJ, Driessler F, Lin S, Allison S, Stehrer B, Lin EJ, Zhang L, Enriquez RF, Wong IP, McDonald MM, During M, Pierroz DD, Slack K, Shi YC, Yulyaningsih E, Aljanova A, Little DG, Ferrari SL, Sainsbury A, Eisman JA, Herzog H. Neuropeptide Y knockout mice reveal a central role of NPY in the coordination of bone mass to body weight. *PLoS One*. 2009;4(12):e8415.
7. Baldock PA, Allison SJ, Lundberg P, Lee NJ, Slack K, Lin EJ, Enriquez RF, McDonald MM, Zhang L, During MJ, Little DG, Eisman JA, Gardiner M, Yulyaningsih E, Lin S, Sainsbury A, Herzog H. Novel role of Y1 receptors in the coordinated regulation of bone and energy homeostasis. *J Biol Chem*. 2007;282(26):19092–102.
8. Baldock PA, Sainsbury A, Couzens M, Enriquez RF, Thomas GP, Gardiner EM, Herzog H. Hypothalamic Y2 receptors regulate bone formation. *J Clin Invest*. 2002;109(7):915–21.
9. Lee NJ, Nguyen AD, Enriquez RF, Doyle KL, Sainsbury A, Baldock PA, Herzog H. Osteoblast specific Y1 receptor deletion enhances bone mass. *Bone*. 2011 Mar 1; 48(3):461–7.
10. Sousa DM, Baldock PA, Enriquez RF, Zhang L, Sainsbury A, Lamghari M, Herzog H. Neuropeptide Y Y1 receptor antagonism increases bone mass in mice. *Bone*. 2012;51(1):8–16.



11. Schwartz MW, Dallman MF, Woods SC. Hypothalamic response to starvation: implications for the study of wasting disorders. *Am J Physiol*. 1995;269 (5 Pt 2): R949–57.
12. Spanswick D, Smith MA, Groppi VE, Logan SD, Ashford ML. Leptin inhibits hypothalamic neurons by activation of ATP-sensitive potassium channels. *Nature*. 1997;390(6659):521–5.
13. Spiegelman BM, Flier JS. Adipogenesis and obesity: rounding out the big picture. *Cell*. 1996;87(3):377–89.
14. Dumont Y, Moysé E, Fournier A, Quirion R. Distribution of peripherally injected peptide YY ([125I] PYY (3–36)) and pancreatic polypeptide ([125I] hPP) in the CNS: enrichment in the area postrema. *J Mol Neurosci*. 2007;33(3):294–304.
15. Wilding JP, Gilbey SG, Bailey CJ, Batt RA, Williams G, Ghatei MA, Bloom SR. Increased neuropeptide-Y messenger ribonucleic acid (mRNA) and decreased neurotensin mRNA in the hypothalamus of the obese (ob/ob) mouse. *Endocrinology*. 1993; 132(5):1939–44.
16. Schwartz MW, Baskin DG, Bukowski TR, Kuijper JL, Foster D, Lasser G, Prunkard DE, Porte D Jr, Woods SC, Seeley RJ, Weigle DS. Specificity of leptin action on elevated blood glucose levels and hypothalamic neuropeptide Y gene expression in ob/ob mice. *Diabetes*. 1996; 45(4):531–5.
17. Stephens TW, Basinski M, Bristow PK, Bue-Valleskey JM, Burgett SG, Craft L, Hale J, Hoffmann J, Hsiung HM, Kriauciunas A, MacKellar W, Rosteck PR Jr, Schoner B, Smith D, Tinsley FC, Zhang X, Heiman M. The role of neuropeptide Y in the antiobesity action of the obese gene product. *Nature*. 1995;377(6549):530–2.
18. Stanley BG, Kyrkouli SE, Lampert S, Leibowitz SF. Neuropeptide Y chronically injected into the hypothalamus: a powerful neurochemical inducer of hyperphagia and obesity. *Peptides*. 1986;7(6):1189–92.
19. Billington CJ, Briggs JE, Harker S, Grace M, Levine AS. Neuropeptide Y in hypothalamic paraventricular nucleus: a center coordinating energy metabolism. *Am J Physiol*. 1994;266 (6 Pt 2): R1765–0.
20. Takeda S, Eleftheriou F, Levasseur R, Liu X, Zhao L, Parker KL, Armstrong D, Ducy P, Karsenty G. Leptin regulates bone formation via the sympathetic nervous system. *Cell*. 2002;111(3):305–17.
21. Sainsbury A, Schwarzer C, Couzens M, Herzog H. Y2 receptor deletion attenuates the type 2 diabetic syndrome of ob/ob mice. *Diabetes*. 2002;51(12):3420–7.
22. Zhang L, Riepler SJ, Turner N, Enriquez RF, Lee IC, Baldock PA, Herzog H, Sainsbury A. Y2 and Y4 receptor signaling synergistically act on energy expenditure and physical activity. *Am J Physiol Regul Integr Comp Physiol*. 2010;299(6):R1618–28.
23. Zhang L, Macia L, Turner N, Enriquez RF, Riepler SJ, Nguyen AD, Lin S, Lee NJ, Shi YC, Yulyaningsih E, Slack K, Baldock PA, Herzog H, Sainsbury A. Peripheral neuropeptide Y Y1 receptors regulate lipid oxidation and fat accretion. *Int J Obes (Lond)*. 2010;34(2): 357–73.
24. Ferrannini E. The theoretical bases of indirect calorimetry: a review. *Metabolism*. 1988;37(3):287–301.

25. Frayn KN. Calculation of substrate oxidation rates in vivo from gaseous exchange. *J Appl Physiol*. 1983;55(2):628–34.
26. McLean JA, Tobin G. *Animal and human calorimetry*. Cambridge: Cambridge University Press; xiii, 338. p. 1987.
27. Shi YC, Lin S, Wong IP, Baldock PA, Aljanova A, Enriquez RF, Castillo L, Mitchell NF, Ye JM, Zhang L, Macia L, Yulyaningsih E, Nguyen AD, Riepler SJ, Herzog H, Sainsbury A. NPY neuron-specific Y2 receptors regulate adipose tissue and trabecular bone but not cortical bone homeostasis in mice. *PLoS One*. 2010;5(6):e11361.
28. Allison SJ, Baldock P, Sainsbury A, Enriquez R, Lee NJ, Lin EJ, Klugmann M, During M, Eisman JA, Li M, Pan LC, Herzog H, Gardiner EM. Conditional deletion of hypothalamic Y2 receptors reverts gonadectomy-induced bone loss in adult mice. *J Biol Chem*. 2006; 281(33):23436–4.
29. Lundberg P, Koskinen C, Baldock PA, Lothgren H, Stenberg A, Lerner UH, Oldenborg PA. Osteoclast formation is strongly reduced both in vivo and in vitro in the absence of CD47/SIRPalpha-interaction. *Biochem Biophys Res Commun*. 2007;352(2):444–8.
30. Trostler N, Romsos DR, Bergen WG, Leveille GA. Skeletal muscle accretion and turnover in lean and obese (ob/ob) mice. *Metabolism*. 1979;28(9):928–33.
31. Bray GA, York DA. Hypothalamic and genetic obesity in experimental animals: an autonomic and endocrine hypothesis. *Physiol Rev*. 1979;59(3):719–809.
32. Chehab FF, Lim ME, Lu R. Correction of the sterility defect in homozygous obese female mice by treatment with the human recombinant leptin. *Nat Genet*. 1996;12(3):318–20.
33. Raposinho PD, Pierroz DD, Broqua P, White RB, Pedrazzini T, Aubert ML. Chronic administration of neuropeptide Y into the lateral ventricle of C57BL/6J male mice produces an obesity syndrome including hyperphagia, hyperleptinemia, insulin resistance, and hypogonadism. *Mol Cell Endocrinol*. 2001;185(1–2):195–204.
34. Baldock PA, Allison SJ, McDonald MM, Sainsbury A, Enriquez R, Little DG, Eisman JA, Gardiner EM, Herzog H. Hypothalamic regulation of cortical bone mass: opposing activity of Y2 receptor and leptin pathways. *J Bone Miner Res*. 2006 Oct; 21(10):1600–7.
35. Lee NJ, Allison S, Enriquez RF, Sainsbury A, Herzog H, Baldock PA. Y2 and Y4 receptor signalling attenuates the skeletal response of central NPY. *J Mol Neurosci*. 2011;43(2):123–31.
36. Hamrick MW, Ding KH, Ponnala S, Ferrari SL, Isales CM. Caloric restriction decreases cortical bone mass but spares trabecular bone in the mouse skeleton: implications for the regulation of bone mass by body weight. *J Bone Miner Res*. 2008;23(6):870–8.
37. Lundberg P, Allison SJ, Lee NJ, Baldock PA, Brouard N, Rost S, Enriquez RF, Sainsbury A, Lamghari M, Simmons P, Eisman JA, Gardiner EM, Herzog H. Greater bone formation of Y2 knockout mice is associated with increased osteoprogenitor numbers and altered Y1 receptor expression. *J Biol Chem*. 2007;282(26):19082–91.
38. Igwe JC, Jiang X, Paic F, Ma L, Adams DJ, Baldock PA, Pilbeam CC, Kalajzic I. Neuropeptide Y is expressed by osteocytes and can inhibit osteoblastic activity. *J Cell Biochem*. 2009;108(3):621–30.

39. Erickson JC, Hollopeter G, Palmiter RD. Attenuation of the obesity syndrome of ob/ob mice by the loss of neuropeptide Y. *Science*. 1996;274(5293):1704–7.
40. Sainsbury A, Schwarzer C, Couzens M, Jenkins A, Oakes SR, Ormandy CJ, Herzog H. Y4 receptor knockout rescues fertility in ob/ob mice. *Genes Dev*. 2002;16(9):1077–88.
41. Baek K, Barlow AA, Allen MR, Bloomfield SA. Food restriction and simulated microgravity: effects on bone and serum leptin. *J Appl Physiol*. 2008;104(4):1086–93.
42. Hoiseth A, Alho A, Husby T. Femoral cortical/cancellous bone related to age. *Acta Radiol*. 1990;31(6):626–7.